

## Chemiluminescence of 1,2-Dioxetane. Reaction Mechanism Uncovered

Luca De Vico,<sup>\*†</sup> Ya-Jun Liu,<sup>\*‡</sup> Jesper Wisborg Krogh,<sup>†</sup> and Roland Lindh<sup>§</sup>

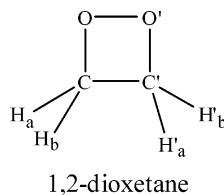
Departments of Theoretical Chemistry and Chemical Physics, Lund University, Chemical Centre, P. O. Box 188, S-221 00 Lund, Sweden and College of Chemistry, Beijing Normal University, Beijing 100875, People's Republic of China

Received: May 25, 2007

The thermal decomposition of 1,2-dioxetane and the associated production of chemiluminescent products, model for a wide range of chemiluminescent reactions, has been studied at the multistate multiconfigurational second-order perturbation level of theory. This study is in qualitative and quantitative agreement with experimental observations with respect to the activation energy and the observed increase of triplet and singlet excited products as substituents are added to the parent molecule. The, previously incomplete, reaction mechanism of the chemiluminescence of 1,2-dioxetane is now rationalized and described as mainly due to a particular form of entropic trapping.

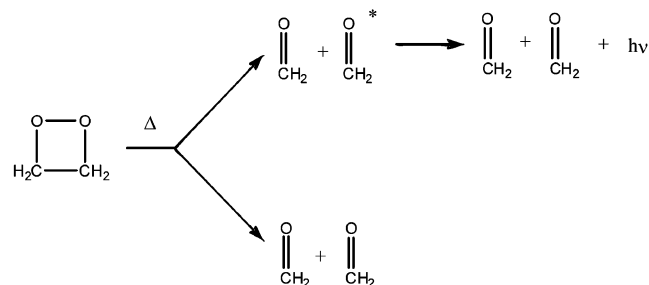
### 1. Introduction

The most spectacular types of chemical reactions are those that produce cold light (chemiluminescence),<sup>1</sup> especially if the process takes place in a living organism (bioluminescence).<sup>2</sup> Do not we all remember the first experience as two fluids after mixture started to emit a mesmerizing greenish light in the darkness of the laboratory, or the first time during a summer night when we as small kids saw our first firefly or glow worm? The mechanism behind these types of chemical reactions have for a long time been of interest to chemists, and a basic understanding of the process exists today—a chemical compound undergoes a thermal decomposition, of which the resulting products are in an excited state, followed by an emission of the excess energy in the form of light. For this to take place with a significant yield in a living organism, we would expect the parent molecule to have bonds which are thermally sensitive, and the produced fragment, which is in the excited state, to be small or rigid to minimize radiationless relaxation. To understand the very details of this process and to possibly explore it to our advantage, the thermal decomposition of 1,2-dioxetane has been the focus of many experimental and theoretical investigations.<sup>3</sup>



The reason for this interest is simple—1,2-dioxetane is, probably, the smallest chemical system capable of chemiluminescence (see Scheme 1). When lightly heated, 1,2-dioxetane decomposes into two formaldehyde fragments. A small fraction of the generated formaldehyde molecules will be in an excited

**SCHEME 1**



state, from which they will return to the ground state by emitting a photon of light. Furthermore, in the luciferin/luciferase light production system of the firefly the bioluminescent process is initiated by an oxidation by molecular oxygen, followed then by the decomposition process. In this respect, 1,2-dioxetane represents the simplest model of the luciferin molecule—the key chemical compound which facilitates the whole process.

Both singlet and triplet pathways can be responsible for the production of the photon of light. In a cornerstone paper, Adam and Baader<sup>4</sup> experimentally measured the activation energies and the yields of singlet and triplet chemiluminescence of 1,2-dioxetane and a series of methyl-substituted compounds. The measured reaction activation energy of the 1,2-dioxetane parent compound was  $22.7 \pm 0.8$  kcal/mol. In addition, the idea that the activation energy for the fundamental-state decomposition represents the rate-determining step for the production of excited singlet or triplet products was supported by experimental evidence from various dioxetane compounds.<sup>5</sup> Furthermore, for the nonsubstituted compound, they found the triplet excitation yield to be small but measurable. However, the triplet excitation yield was found to be definitely larger than the singlet yield ( $\phi^t = 0.0024 \pm 0.006$  einstein/mol,  $\phi^s = (0.0031 \pm 0.0006) \times 10^{-3}$  einstein/mol). Even within the, eventual, errors of the experimental method, the presence of a preference for the triplet pathway is undeniable. In fact, along the series of studied compounds, while the excited species yields become larger following the number of methyl substituents, the triplet/singlet yield ratio always exceeds 140.

\* Corresponding author. E-mail: luca.de\_vico@teokem.lu.se (L.D.V.); yajun.liu@bnu.edu.cn (Y.-J.L.).

† Department of Theoretical Chemistry, Lund University.

‡ Beijing Normal University.

§ Department of Chemical Physics, Lund University.

The generally accepted mechanism for the reaction is the so-called asynchronous concerted (or merged) mechanism.<sup>4,6</sup> It states that the first part of the chemiluminescent reaction should be concerted: the O–O' bond will extend, while the C–C' bond also undergoes some stretching. This is followed by a biradical phase (where the O–O' bond is broken) prior to the decomposition (C–C' bond breaking) into the excited-states products.

To understand the dissociation process of 1,2-dioxetane, it is useful to consider the well-described ring-opening reaction of the isoelectronic cyclobutane. The ring opening of cyclobutane goes through an intermediate, the 1,4-tetramethylene biradical. The existence of such an intermediate has been proven by femtosecond spectroscopy.<sup>7</sup> First theoretically<sup>8</sup> and then experimentally<sup>9</sup> it has been demonstrated that the tetramethylene biradical lifetime is controlled by an entropic trapping process (vide infra). Considering such a mechanism will be, then, necessary in order to define the reaction mechanism of also 1,2-dioxetane. In the tetramethylene case, only two potential states are involved, one singlet and one triplet. The situation for 1,2-dioxetane is more complicated. In addition to the spin coupling of the two radical electrons, for each C–O moiety one has to consider also the internal excitation between the oxygen doubly occupied and the singly occupied p orbitals. We will show how such an increased number of possible states affects the entropic trapping process.

The theoretical work on the 1,4-tetramethylene biradical showed, also, how a multiconfigurational reference perturbation theory (CASPT2) treatment is indispensable in order to fully describe the reaction route. Previous theoretical studies of the 1,2-dioxetane dissociation employing both a complete active space CASSCF method, coupled with a multireference MP2 correction of the energetic,<sup>10</sup> and a density functional approach (DFT)<sup>11</sup> failed to correctly access the activation barrier and/or identify the entropic trap that facilitates the chemiluminescence. Also more recent work,<sup>12</sup> mostly about variously substituted dioxetanes, does not possess the accuracy needed by the peculiarities of the system. Namely, a multiconfigurational approach that takes into account the four singlets and four triplet states is essential, as will be clear in the following paragraphs. Hence, we decided to examine the thermal decomposition of 1,2-dioxetane with state-of-the-art and novel computational methods. The main goals of this study were to have an accurate reproduction of the activation energy barrier and a complete description of the routes leading to the formation of fundamental, excited singlet, and excited triplet products.

## 2. Computational Methods

Geometry optimization and minimum energy path searches were carried out using MS-CASPT2//CASSCF and MS-CASPT2//MS-CASPT2 PES evaluation techniques.

For the MS-CASPT2//CASSCF part, geometry optimizations and minimum energy path (MEP) searches were performed by evaluating energies and gradients (analytically) of the multi-reference CASSCF<sup>13</sup> PES, calculated using a four roots equal weights state average wave function for states of singlet and triplet multiplicity. This will allow for a complete description of all possible states in which the lone-pair and radical electrons are distributed in the appropriate orbitals on the oxygen atoms. The ANO-RCC<sup>14</sup> basis set with a contraction [4s3p2d1f] for carbon and oxygen atoms, and [3s2p1d] for the hydrogens, was used in all calculations. An active space of 12 electrons in 10 orbitals was chosen. The active orbitals comprise the C–C', C–O, C'–O', and O–O' σ bonding and antibonding orbitals, plus the two oxygen lone-pair orbitals. Along the reaction path,

O–O' and C–C' bond breaking causes some σ/σ\* orbitals to change nature and become first lone pairs and then π/π\*. MEP searches were conducted as constrained optimizations on hyperspheres.<sup>15</sup> MEP searches were done in two possible ways: (i) “downward” and (ii) “upward”. In i the center of the hypersphere was set as the structure optimized at a previous step (or a starting geometry for the first step), and the radius length was fixed. In ii the center of the hypersphere was fixed to be the starting geometry, and the first radius was set to reach a previously optimized target structure. Subsequent optimizations employed shorter radii. The energies of the so-obtained geometries were reevaluated, applying a multistate multiconfigurational reference perturbation theory correction (MS-CASPT2),<sup>16</sup> using the average four singlet and triplet CASSCF wave functions as a reference. For some structures, the use of an imaginary shift of 0.1 was necessary, in order to remove some intruder-state problems.<sup>17</sup>

For the MS-CASPT2//MS-CASPT2 part, the structures were directly optimized on the MS-CASPT2 PES (singlet or triplet depending on the state of interest) using the same average CASSCF reference functions as before. Energy gradients were evaluated by using a numerical method. MEP searches were performed in a downward manner. To speed up the process, structures previously optimized at the CASSCF level of theory were used, when possible, as starting geometries.

In all MS-CASPT2 calculations, core orbitals of non-hydrogen atoms were frozen and a standard IPEA modification of the zeroth-order Hamiltonian with value 0.25 was employed.<sup>18</sup>

All calculations were performed using the MOLCAS 6.3 suite of programs.<sup>19</sup>

## 3. Results and Discussion

First we will present the MS-CASPT2//MS-CASPT2 MEP over S<sub>0</sub> PES, giving account of the activation energy barrier. The analysis will show that the entire four singlet and four triplet states manifold becomes degenerate when the molecule is in the vicinity of the transition state corresponding to the O–O' bond rupture. The following section will then present the MS-CASPT2//CASSCF T<sub>1</sub> and S<sub>1</sub> MEPs. These are the possible paths for the production of two formaldehydes, one of which in an excited state. The last section will then offer an analysis of the molecular modes involved in the reaction coordinate, along with an alternative MS-CASPT2//CASSCF S<sub>0</sub> MEP.

As mentioned in the Introduction, it will be indispensable to interpret the data in view of an entropic trapping mechanism. Both the theoretical<sup>8</sup> and experimental<sup>9</sup> works demonstrated how, although any classical barrier toward dissociation of the 1,4-tetramethylene biradical was absent, the species was entropically trapped, corresponding to a dissociation barrier of 5 kcal/mol. Such trapping is “tuned” by the number of degrees of freedom available for the molecular fragments interested by the reaction. Such a relationship is direct: the greater the number of degrees of freedom, the longer is the trapping. Clearly, increasing the number of substituents on the 1,2-dioxetane molecule increases the number of degrees of freedom. We will see how such an event is connected to the increased production of excited-state species. A plausible explanation of the preferred production of triplet instead of singlet excited formaldehyde will be offered.

**3.1. MS-CASPT2//MS-CASPT2 S<sub>0</sub> MEP.** The reactant minimum and the transition state (TS S<sub>0</sub>) for the thermal dissociation of 1,2-dioxetane were found by geometry optimization at the CASSCF level of theory. After MS-CASPT2 energetic correction, the computed energy difference was 23.5

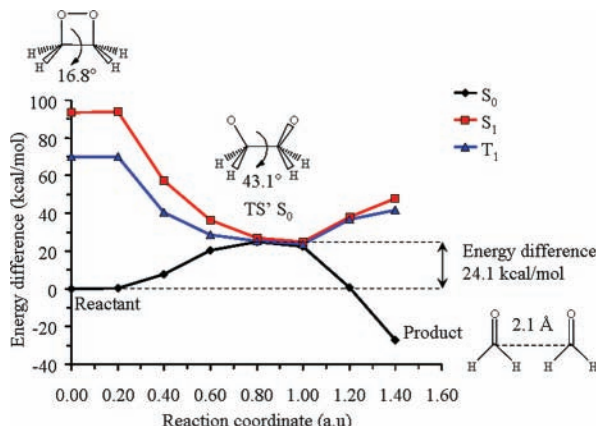


**Figure 1.** Computed MS-CASPT2//MS-CASPT2  $S_0$  MEP. Only  $S_0$  (black full line and diamonds),  $S_1$  (red line and squares), and  $T_1$  (blue line and triangles) are reported. Figure 8S in the Supporting Information reports the MEP comprehensive of all computed states. The dashed lines and the double arrow highlight the energy difference between the reactants and the transition state ( $TS' S_0$ ) that gives rise to the activation energy barrier. For the reactant and  $TS' S_0$  structures the  $O-C-C'-O'$  dihedral angle value is given in degrees; the  $C-C'$  distance in angstroms of the last MEP point is also reported.

kcal/mol. With or without thermal correction, this value agrees with the experimental value of the activation energy barrier ( $22.7 \pm 0.8$  kcal/mol). A downward MEP at the average CASSCF level of theory connecting these two structures and toward dissociation products was computed with some technical difficulties, but it is not reported here because it showed some un-physical behavior. See Figure 7S in the Supporting Information. We decided, then, to increase the level of theory, and we recalculated the  $S_0$  MEP by exploring directly the MS-CASPT2 PES. It is known that sometimes a MS-CASPT2//CASSCF treatment alone could not be sufficient<sup>20</sup> in order to describe a difficult situation, even when the quality of the CASSCF reference wave function is good. This profile is presented in Figure 1. The downward MEP search toward the products species was interrupted as soon as the two molecules were clearly separated.

The calculated energy difference between the reactant minimum and  $TS' S_0$  is 24.1 kcal/mol, in agreement with the experimental activation barrier. A full description of the reaction coordinate and its analysis is given in section 3.3. Just to notice here that twisting around the  $C-C'$  bond and, consequently, stretching the  $O-O'$  bond leads the molecule from the reactant minimum to a transition state ( $TS' S_0$ ). After that the  $C-C'$  bond stretching comes into action and leads the molecule toward the dissociation products.

At  $TS' S_0$  all considered states, both singlet and triplet, are comprised within 13 kcal/mol. At the next MEP point (at 1.00 au), the energetic gap between the lowest and the highest considered state is further reduced to less than 6 kcal/mol. See Table 4S in the Supporting Information. It is clear that in this part of the reaction path there is a strong interaction between all the considered states.

The MS-CASPT2//MS-CASPT2  $S_0$  MEP agrees with the MS-CASPT2//CASSCF results (Figure 7S of the Supporting Infor-

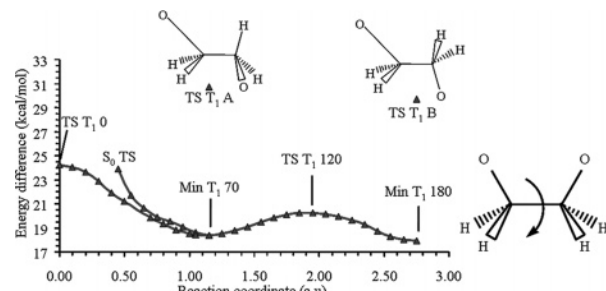


**Figure 2.** MS-CASPT2//CASSCF  $T_1$  potential energy surface. Two transition states ( $TS T_1 0$  and  $TS T_1 120$ ) and two minima ( $Min T_1 70$  and  $Min T_1 180$ ) are shown, along with the MEP connecting them. In addition, the MEP on the  $T_1$  PES from  $TS S_0$  is presented. The two transition-states structures ( $TS T_1 A$  and  $TS T_1 B$ ) share nearly the same torsional angle around the  $C-C'$  bond as the two minima, and for this reason are reported above them (at their proper relative energy), even if they are not related to the reaction coordinate used along the abscissa. The energy difference is calculated with respect to the MS-CASPT2  $S_0$  energy of the CASSCF optimized reactant minimum, in order to maintain consistency. The complete set of computed states is reported in Figure 9S in the Supporting Information.

mation) in terms of PES shape, energetic, and molecular structures. For this reason, since no other unphysical behaviors were found, the next presented MEPs were performed at the MS-CASPT2//CASSCF level of theory.

**3.2. MS-CASPT2//CASSCF  $T_1$  MEP and  $S_1$ .** Given the small gap between  $S_0$  and  $T_1$  found at the CASSCF optimized  $TS S_0$ , we decided to take that structure as a starting geometry for a MEP search along the  $T_1$  PES. A real interstate crossing (ISC) between  $S_0$  and  $T_1$  was, anyway, located close to this structure (within 0.1 au), and the first points along the  $T_1$  MEP show that these two states are still nearly degenerate (see Figure 9Sa in the Supporting Information). This means that there should be a large and spread area of degeneracy or near-degeneracy between  $S_0$  and  $T_1$  in the proximity of the transition state. More details on this aspect will also be given in the next section. The  $T_1$  MEP is mainly characterized by the continuation of the torsional rotation around the  $C-C'$  bond and ends in a minimum of the PES. The  $T_1$  PES is constituted by a valley spanning the torsion around the  $C-C'$  bond: it is characterized by the total presence of three transition states and three minima. We explored the torsion from 0 to 180°, since obviously the rest is simply mirrored. Figure 2 reports the MS-CASPT2//CASSCF  $T_1$  PES and the  $T_1$  MEP from  $TS S_0$ .

Almost the entire  $T_1$  valley is energetically accessible since  $TS T_1 120$  is lower in energy with respect to  $TS S_0$ ; however,  $TS T_1 0$  is slightly higher in energy. For any structure along the  $T_1$  PES valley, carbon–oxygen bonds are of the same length, as well as the pyramidalization at the carbon atoms is conserved. By breaking this symmetry, it is possible to reach a ridge leading to the dissociation into two formaldehyde molecules, one of which is an excited state. By these means,  $TS T_1 A$  and  $TS T_1 B$  (see Figure 2) were found. Table 1 reports their main geometrical parameters. Since the two carbon atoms are now clearly different one from another, one has to remember that there exist two mirror structures of each  $TS T_1$ , one for each side of the valley. Furthermore, since the valley extends itself

**TABLE 1: Main Structural Properties of  $TS T_1 A$  and  $TS T_1 B$**

	$TS T_1 A$	$TS T_1 B$	$TS T_1 A$	$TS T_1 B$
$O-C-C'-O'$ dihedral angle (deg)	79.3	179.9	$C-C'$ distance (Å)	2.017
$C-O$ distance (Å)	1.267	1.267	$C$ pyramidalization <sup>a</sup> (deg)	6.1
$C'-O'$ distance (Å)	1.369	1.372	$C'$ pyramidalization <sup>a</sup> (deg)	22.4

<sup>a</sup> Computed as difference between 360° and the sum of the bond angles  $O-C-H_a$ ,  $O-C-H_b$ , and  $H_a-C-H_b$ .

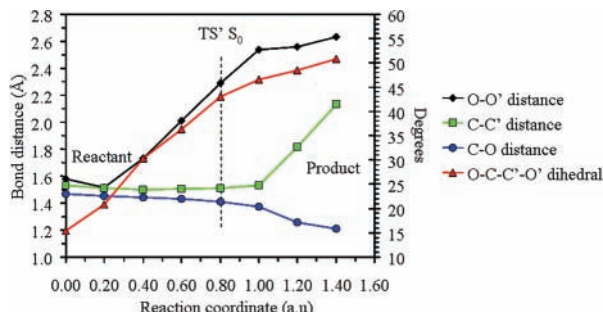


**Figure 3.** Structural changes along the MS-CASPT2//MS-CASPT2  $S_0$  MEP reported in Figure 1. The dashed line highlights the position of the transition-state structure  $TS' S_0$  along the reaction coordinate.

on the full  $360^\circ$  of torsion around the  $C-C'$  bond, there will be a mirror structure of Min  $T_1$  70 and the corresponding transition-state mirror of  $TS T_1$  A. This will sum up to six transition states leading out of the  $T_1$  valley.

The exploration of the  $S_1$  PES turned out to be more difficult, since it has a strong degeneracy with  $S_0$ . The same stationary points as on the  $T_1$  PES were located (Min  $S_1$  70, Min  $S_1$  180,  $TS S_1$  0,  $TS S_1$  120,  $TS S_1$  A, and  $TS S_1$  B). To connect these points through a trivial MEP search, however, was found to be impossible, since the optimizer flipped randomly from the  $S_1$  to the  $S_0$  state, and then followed this surface down to the fundamental reaction path. Actually, Min  $S_1$  70 and Min  $S_1$  180 were optimized as  $S_0$  minima, since  $S_0$  and  $S_1$  are completely degenerate at these structures. Anyway, the same features of the  $T_1$  PES are expected.

**3.3. Reaction Coordinate Analysis and Discussion. Reaction Coordinate Modes.** As seen in the previous sections, the reaction coordinate of the described MEPs is mainly constituted by these modes:  $O-O'$  and  $C-C'$  bonds stretching,  $O-C-C'-O'$  dihedron torsion, asymmetric  $[O-C/O'-C']$  bonds stretching, and asymmetric  $[C/C']$  pyramidalization. Figure 3 presents a more detailed analysis of the first four modes along the MS-CASPT2//MS-CASPT2  $S_0$  MEP of Figure 1.

As can be seen in Figure 3, after  $TS' S_0$  the MEP takes a turn on the PES: the  $O-O'$  distance increasing and the torsion around the  $O-C-C'-O'$  dihedron nearly stopping, while the increase of the  $C-C'$  distance comes into action. This ultimately leads to the production of two formaldehyde molecules, signaled by the shortening of the carbon oxygen bonds. At this point we have to remember that the computed MEP path represents the reaction in the absence of any kinetic energy, while in reality the true reaction path, to some degree, will be ballistic. Hence, the possibility of an entropic trapping similar to that for the tetramethylene biradical has to be carefully considered. What would be the consequences if the reaction continued along the torsional mode? Section 3.2 already suggested that this is of interest—the torsional mode is the principal internal coordinate of the  $T_1$  MEP. We decided to investigate this possibility further.

**Entropic Trapping.** We computed an alternative MS-CASPT2//CASSCF “upward” MEP starting from  $TS S_0$ , as reported in Figure 4. The aim of this path was made to point toward a twisted structure ( $Min S_1$  70, where one has to remember that  $S_0$  and  $S_1$  are degenerate). Figure 4 shows that, after the transition-state structure, it is also possible to follow a barrierless route along a reaction coordinate mainly constituted by only the torsional mode and that, along this path,  $S_0$ ,  $S_1$ , and  $T_1$  potential energy surfaces are degenerate or close to degeneracy, giving way to infinite possibilities for the molecule to change state.

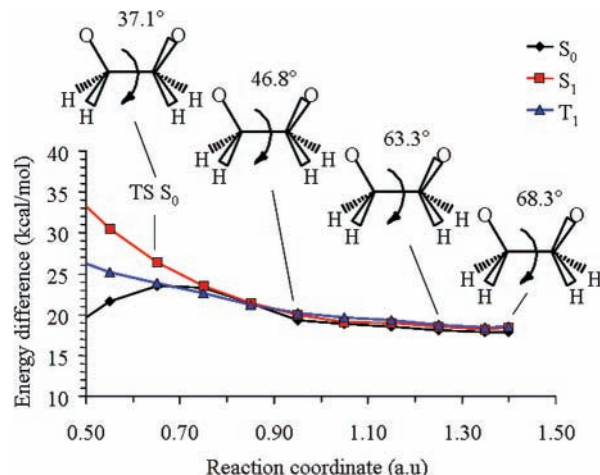


**Figure 4.** MS-CASPT2//CASSCF  $S_0$  alternative path from  $TS S_0$ . Only  $S_0$  (black line and diamonds),  $S_1$  (red line and squares), and  $T_1$  (blue line and triangles) are reported. Figure 10S in the Supporting Information reports the MEP comprehensive of all computed states. The energy difference is calculated as in Figure 2. The path before  $TS S_0$  is the same as in Figure 7S. For  $TS S_0$  and selected points along the MEP, the value of the dihedral angle  $O-C-C'-O'$  in degrees is reported. For these structures, the values of the  $C-O$  ( $C'-O'$ ) bond are 1.438, 1.416, 1.413, and 1.413 Å; the  $C-C'$  bond are 1.536, 1.545, 1.546, and 1.546 Å; and the  $O-O'$  bond are 2.262, 2.664, 2.958, and 3.016 Å, respectively.

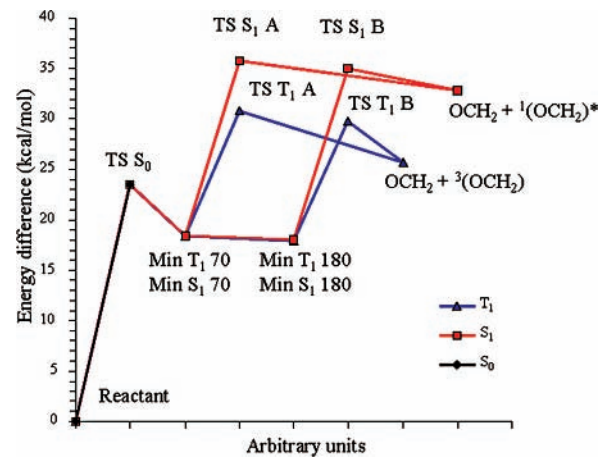


**Figure 5.** Relative energies of the stationary points on the PES, relative to the production of  $T_1$  or  $S_1$  excited formaldehyde molecules.

The path reported in Figure 4 represents the entropic trapping for the 1,2-dioxetane molecule, a barrier-less almost flat region of the PES. This path is accessed because after the transition state the molecule is “ballistic”, and thus remains along the torsional mode. Vibrational mode redistribution is needed in order for the molecule to slide onto the path reported in Figure 1. As stated in the Introduction, due to the abundance of possible combinations for the electrons in the p orbitals of the oxygen atoms, a very peculiar entropic trapping is encountered. In fact, as a result of the degeneracy of the states, the entropic trapping is also a crossing seam<sup>21</sup> region.

**Dissociation Products Control.** This situation strongly affects the fate of the dissociating molecule, since the entropic trapping significantly increases the molecule lifetime in a region where state crossing is possible. As stated at the beginning of section 3, the entropic trapping is governed by the number of degrees of freedom available to the molecule or the molecular moiety. Clearly, the addition of substituents on the carbon atoms increases the number of degrees of freedom of the molecule.

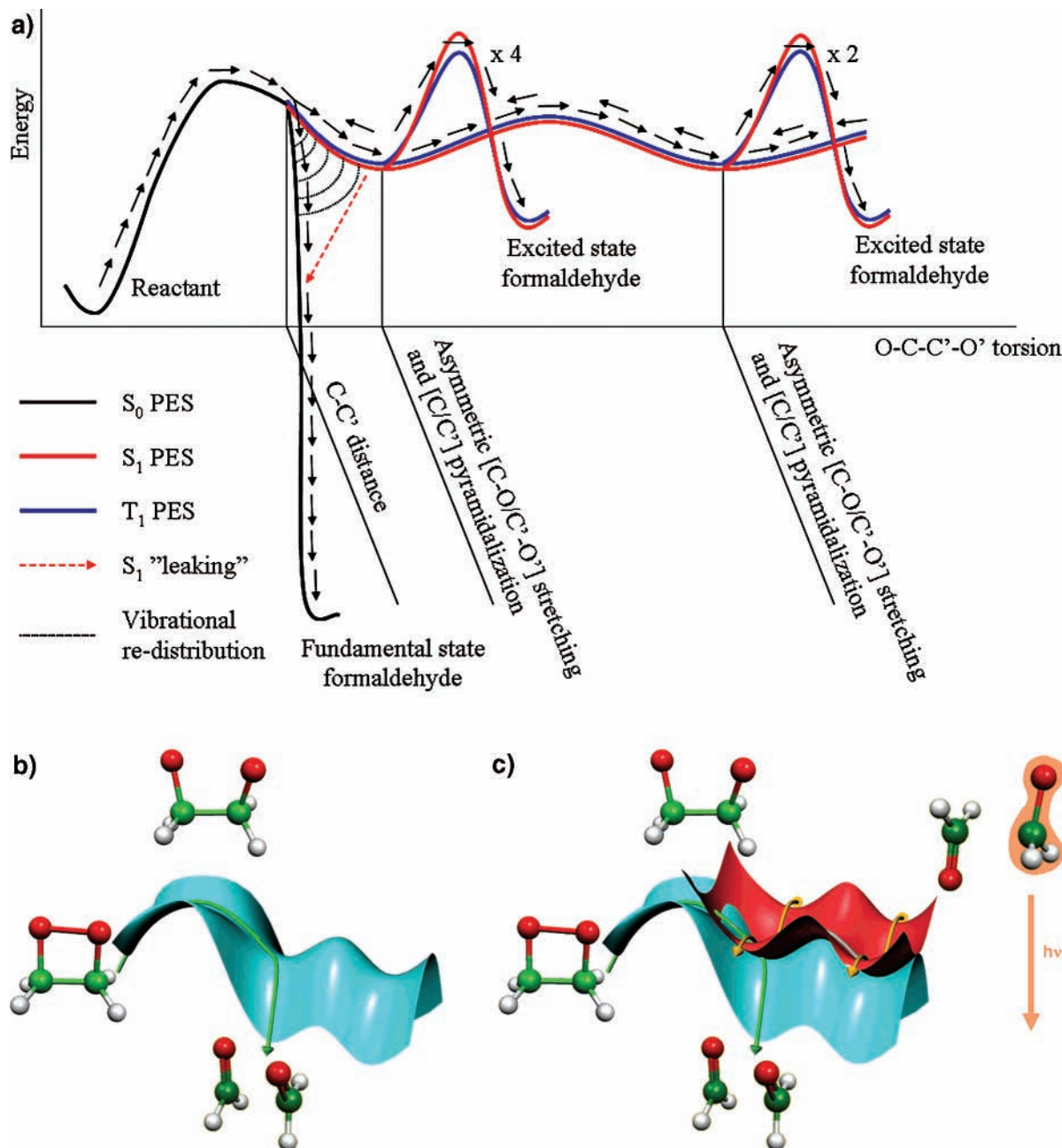


**Figure 6.** (a) Schematization of the possible routes for 1,2-dioxetane to produce fundamental- or excited-state formaldehyde molecules. The main reaction coordinate is represented by the torsion around the O—C—C'—O' dihedron. The perpendicular routes to reach the final products are also reported: C—C' bond stretching to reach fundamental-state formaldehyde and asymmetric [C—O/C'—O'] bond stretching and [C/C'] pyramidalization to produce excited-state formaldehyde. The dotted lines stand for the re-distribution of vibrational energy following the first transition-state structure. The dashed arrow represents the phenomenon of production of fundamental-state formaldehyde from the  $S_1$  PES through an intersection with  $S_0$ . Since the tentative 3D representation, energies are not in scale. (b) Pictorial representation of the dissociation process on  $S_0$  and (c) also on the excited states  $S_1$  and  $T_1$ , along with the, relative, dissociation products.

This, in turn, will increase the time spent in the entropic trapping, and therefore the possibility for the molecule to cross onto the  $S_1$  or  $T_1$  PES. This mechanism represents the explanation for the increased production of excited-state (both singlet and triplet) products upon addition of methyl substituents. The passage on  $T_1$  is assured by the high spin-orbit coupling between the first singlet and triplet states. In the Supporting Information, Table 3S reports such coefficients for a randomly selected point along the path of Figure 4. The situation is similar along the entire path. We remember, though, that since an entire section of the path is degenerate, it is not possible to clearly define which point has the maximum probability of crossing. The only

unambiguous element is the existence of the large area of degeneracy on the PES.

The entropic trapping does not only regulate the branching between fundamental and excited-state products, it is also essential to the formation of the excited-state products. A further analysis of the PES is needed in order to appreciate this statement. To reach the entropic trapping region, the molecule has to overcome the energy barrier represented by the O—O' bond breaking transition state, calculated as 23.5 kcal/mol at the MS-CASPT2//CASSCF level. While in the entropic trap, the molecule can cross to  $S_1$  or  $T_1$ , shifting to the surface depicted in Figure 2. From the  $T_1$  ( $S_1$ ) PES valley, passing

through TS T<sub>1</sub> A or TS T<sub>1</sub> B (TS S<sub>1</sub> A or TS S<sub>1</sub> B), the molecule will dissociate into two formaldehyde molecules, one of which in an excited state. Each of these transition states is higher in energy than TS S<sub>0</sub>. See Figure 5. Even after an extensive search, it has not been possible to locate any other transition state lower in energy. In any case, any transition state could not be lower in energy than the final product minima. The minima for the dissociated excited-state products were, indeed, located at higher energy than TS S<sub>0</sub>, as depicted in Figure 5.

Together with the minimum for the fundamental-state dissociated products, the computed vertical excitation and adiabatic emission energies are in agreement with theoretical<sup>22</sup> and experimental<sup>23</sup> data for the monomer. See Table 2S in the Supporting Information.

This finding forces one to reconsider the experimental evidence that production of fundamental and excited-state dissociation products is due to a shared rate-determining step.<sup>4,5</sup> For substituted species it is possible that the relative energies of the first transition state and the excited-state products are different. On the other hand, for all compounds accounted by Adam and Badeer,<sup>4</sup> so including 1,2-dioxetane, the energy barrier associated with the first transition state is reported to regulate the entire process. Then, again, in the same article it is stressed that the production of excited-state formaldehyde is an endothermic process and already available thermochemical estimates<sup>24</sup> put the excited formaldehyde molecules at higher energy than the experimental barrier. To explain the inconsistency between the experimental findings and the transition-states relative energies, then something more must be taken into consideration. The uncommon feature of the thermochemical dissociation of 1,2-dioxetane is, obviously, the entropic trap. It is natural to look to it in order to explain the rate-determining step experimental finding against the relative energy levels of the transition states. The action of the entropic trap resides more on entropic effects rather than potential energy only, as the rest of the path. There is, then, a discontinuity between a potential energy driven path and an entropy driven path. In our opinion, this discontinuity should be accounted as the cause for the blurring of the kinetic data. The mechanism at the base of such discrepancy and its consequences on the excited products yields will be a matter of further investigations.

The analysis of the transition states relative to the production of excited-state products reveals also that those relative to the triplet PES are around 5 kcal/mol lower in energy than those of the singlet PES. See Figure 5 and Table 4S in the Supporting Information. Since along the PES of Figure 2 there are regions of (near) degeneracy between T<sub>1</sub> (S<sub>1</sub>) and S<sub>0</sub>, it is possible for the molecule to cross back onto the fundamental state and recoil to the fundamental-state products. Since the barrier to the dissociation on the singlet surface is higher than that on the triplet surface, molecules will have more possibilities to cross back to S<sub>0</sub>. This explains why, experimentally, the formation of triplet excited formaldehyde has a higher yield than for the singlet species.

Another consequence of the transition-states' relative energies is that they suggest the possibility for a biradical species to exist on S<sub>1</sub> or T<sub>1</sub>. The presence of such compounds has been quite debated.<sup>3,4,10,12</sup> The main experimental evidence is against such existence, since they have not been really detected. We can think of a possible explanation. The path presented in Figure 2 reports only the T<sub>1</sub> energies. The whole of the computed states is presented in Figure 9Sa in the Supporting Information. There it can be seen that, again, the situation is quite degenerate. Such concomitance of different (nearly) overlapping states could

generate a transient species with an average diffuse electron distribution, which could foul traditional methods for radical detection. Also in this case, further investigations will be done.

#### 4. Conclusions

We have explored various reaction paths of thermal decomposition of 1,2-dioxetane by means of MS-CASPT2//CASSCF and MS-CASPT2/MS-CASPT2, both on the fundamental S<sub>0</sub> state as well as on the S<sub>1</sub> and T<sub>1</sub> excited-states PES. Through these means we were able to reproduce the activation energy barrier of the reaction in agreement with the experimental data. In addition, we gave reasons for the rate-determining step of the reaction, the increased production of excited-state species following substituents methylation, and the larger production of triplet over singlet excited species. The main results of the analysis of the computed paths are schematized in Figure 6.

After the O—O' bond breaking transition state, the nature of the vibrational mode most involved in the reaction coordinate guides the molecule toward the production of fundamental-state formaldehyde or toward the T<sub>1</sub> or S<sub>1</sub> potential energy surfaces. The molecules should be able to slide between the two paths, in an entropically trapped region, depending on the redistribution of the vibrational modes (dotted lines in Figure 6a). We argued that, likely, this choice could be tuned by the presence of substituents, which will increase the time spent in the entropic trap.

If the molecule remains along the torsional coordinate, it will then find itself on the S<sub>1</sub> or T<sub>1</sub> surface (Figure 6c), since both are energetically accessible. We argued that, given the difference in energy between TS T<sub>1</sub> A/B and TS S<sub>1</sub> A/B, it is easier for a molecule on the S<sub>1</sub> PES to drop back onto the S<sub>0</sub> surface (S<sub>1</sub> "leaking", dotted red line in Figure 6a) than for a molecule on the T<sub>1</sub> PES. In our view, these differences should account for the different production of excited species, in favor of the triplet one.

The entropic trap constitutes the novelty and the most interesting aspect of the computed paths. It regulates the outcome of the dissociation reaction in three ways. First of all, it prevents the molecule from fast decaying toward the, quite exothermic, fundamental-state dissociation channel. Instead, some molecules are given enough time to span other routes. Second, it constitutes the way to access the S<sub>1</sub> and T<sub>1</sub> potential energy surfaces, given its dual nature of the crossing seam. Finally, somehow it prompts the molecule toward the excited-state dissociation channel, which, otherwise, would be inaccessible, as the rate-determining step seems to suggest. The origin of this last effect, likely, resides onto the discontinuity between potential energy driven and entropy driven paths, whose consequences are, likely, to confuse kinetic data. Anyway, this last aspect remains a matter of open discussion.

**Acknowledgment.** The authors thank LUNARC computer centre of Lund University and SNAC for granted computational time. L.D.V. acknowledges a grant from the Foundation BLANCEFLOR Boncompagni-Ludovisi née Bildt. Y.-J.L. acknowledges funding from the National Natural Science Foundation of China (Grant No. 20673012).

**Supporting Information Available:** Complete reference 19, Figures 7S–10S, one table with computed and experimental energy differences for the dissociated species (Table 2S), one table with spin-orbit coupling coefficients for a point of Figure 4, one table with computed energy data (Table 4S), and one table with Cartesian coordinates (Table 5S) of the various

structures discussed in the text. This material is available free of charge via the Internet at <http://pubs.acs.org>.

## References and Notes

- (1) Braslavsky, S. E.; Houk, K. N.; Verhoeven, J. W. *Pure Appl. Chem.* **1996**, *68*, 2223–2286.
- (2) Kaplan, N. P.; Colowick, N. P.; DeLuca, M. A., Eds. *Bioluminescence and Chemiluminescence*; Academic Press: New York, 1978; Vol. 57. Adam, W., Cilento, G., Eds. *Chemical and Biological Generation of Excited States*; Academic Press: New York, 1982; Vol. 25.
- (3) Adam, W.; Trofimov, A. V. In *The Chemistry of Functional Groups, Peroxides*; Rappoport, Z., Ed.; John Wiley & Sons: New York, 2005; Vol. 2, pp 1171–1210 (for a review on recent developments on dioxetane chemistry and references therein for a list of reviews onto the historical development of research in this field).
- (4) Adam, W.; Baader, W. J. *J. Am. Chem. Soc.* **1985**, *107*, 410–416.
- (5) Wilson, T.; Schaap, A. P. *J. Am. Chem. Soc.* **1971**, *93*, 4126–4136. Steinmetzer, H.-C.; Yekta, A.; Turro, N. J. *J. Am. Chem. Soc.* **1974**, *96*, 282–284.
- (6) Turro, N. J.; Lechtken, P. *J. Am. Chem. Soc.* **1973**, *95*, 264–266. Murphy, S.; Adam, W. *J. Am. Chem. Soc.* **1996**, *118*, 12916–12921.
- (7) Pedersen, S.; Herek, J. L.; Zewail, A. H. *Science* **1994**, *266*, 1359–1364. Polanyi, J. C.; Zewail, A. H. *Acc. Chem. Res.* **1995**, *28*, 119–132.
- (8) Moriarty, N. W.; Lindh, R.; Karlström, G. *Chem. Phys. Lett.* **1998**, *289*, 442–450.
- (9) De Feyter, S.; Diau, E. W.-G.; Scala, A. A.; Zewail, A. H. *Chem. Phys. Lett.* **1999**, *303*, 249–260.
- (10) Wilsey, S.; Bernardi, F.; Olivucci, M.; Robb, M. A.; Murphy, S.; Adam, W. *J. Phys. Chem. A* **1999**, *103*, 1669–1677.
- (11) Tanaka, C.; Tanaka, J. *J. Phys. Chem. A* **2000**, *104*, 2078–2090.
- (12) Bastos, E. L.; Baader, W. J. *ARKIVOC (Gainesville, FL, U.S.)* **2007**, *8*, 257–272.
- (13) Roos, B. O. In *Ab Initio Methods in Quantum Chemistry-II*; Lawley, K. P., Ed.; Advances in Chemical Physics; John Wiley & Sons: New York, 1987; Vol. 69, pp 399–446.
- (14) Roos, B. O.; Lindh, R.; Malmqvist, P.-Å.; Veryazov, V.; Widmark, P.-O. *J. Phys. Chem. A* **2004**, *108*, 2851–2858.
- (15) De Vico, L.; Olivucci, M.; Lindh, R. *J. Chem. Theory Comput.* **2005**, *1*, 1029–1037.
- (16) Finley, J.; Malmqvist, P.-Å.; Roos, B. O.; Serrano-Andrés, L. *Chem. Phys. Lett.* **1998**, *288*, 299–306.
- (17) Forsberg, N.; Malmqvist, P.-Å. *Chem. Phys. Lett.* **1997**, *274*, 196–204.
- (18) Ghigo, G.; Roos, B. O.; Malmqvist, P.-Å. *Chem. Phys. Lett.* **2004**, *396*, 142–149.
- (19) Andersson, K.; et al. *MOLCAS*, Version 6.3; Lund University: Lund, Sweden, 2004. Veryazov, V.; Widmark, P.-O.; Serrano-Andrés, L.; Lindh, R.; Roos, B. O. *Int. J. Quantum Chem.* **2004**, *100*, 626–635.
- (20) Merchán, M.; Serrano-Andrés, L. In *Computational Photochemistry*; Olivucci, M., Ed.; Elsevier: Amsterdam, 2005; pp 35–91.
- (21) Atchity, G. J.; Xantheas, S. S.; Ruedenberg, K. *J. Chem. Phys.* **1991**, *95*, 1862–1876.
- (22) Bruna, P. J.; Hachey, M. R. J.; Grein, F. *J. Phys. Chem.* **1995**, *99*, 16576–16585. Hachey, M. R. J.; Bruna, P. J.; Grein, F. *J. Phys. Chem.* **1995**, *99*, 8050–8057. Merchán, M.; Roos, B. *Theor. Chim. Acta* **1995**, *92*, 227–239.
- (23) Staley, R. H.; Harding, L. B.; Goddard, W. A., III; Beauchamp, J. L. *Chem. Phys. Lett.* **1975**, *36*, 589–593. Clouthier, D. J.; Ramsay, D. A. *Ann. Rev. Phys. Chem.* **1983**, *34*, 31–58. Walzl, K. N.; Koerting, C. F.; Kuppermann, A. *J. Chem. Phys.* **1987**, *87*, 3796–3803.
- (24) O’Neal, H. E.; Richardson, W. H. *J. Am. Chem. Soc.* **1970**, *2*, 6553–6557. O’Neal, H. E.; Richardson, W. H. *J. Am. Chem. Soc.* **1971**, *93*, 1828.